

# New linear and layered amine-templated lanthanum sulfates

Thierry Bataille\* and Daniel Louër

Laboratoire de Chimie du Solide et Inorganique Moléculaire, UMR 6511 CNRS, Institut de Chimie, Université de Rennes I,  
Avenue du Général Leclerc, Rennes Cedex 35042, France

Received 5 August 2003; received in revised form 22 October 2003; accepted 26 October 2003

## Abstract

Two new amine-templated lanthanum sulfates have been synthesized hydrothermally and structurally characterized by single-crystal X-ray diffraction.  $\text{La}(\text{C}_4\text{H}_{16}\text{N}_3)(\text{SO}_4)_3 \cdot \text{H}_2\text{O}$  crystallizes with triclinic symmetry, space group  $P\bar{1}$  [ $a = 8.2800(1) \text{ \AA}$ ,  $b = 9.5755(2) \text{ \AA}$ ,  $c = 10.4439(2) \text{ \AA}$ ,  $\alpha = 105.689(1)^\circ$ ,  $\beta = 102.844(1)^\circ$ ,  $\gamma = 104.372(1)^\circ$ ,  $V = 734.12(2) \text{ \AA}^3$ ,  $Z = 2$ ]. It displays a one-dimensional crystal structure, based on lanthanum atoms connected by the sulfate groups arranged in an helical manner.  $\text{La}_2(\text{H}_2\text{O})_4(\text{C}_6\text{H}_{14}\text{N}_2)_2(\text{SO}_4)_5 \cdot 5\text{H}_2\text{O}$  crystallizes with orthorhombic symmetry, space group  $Pna2_1$  [ $a = 13.5972(1) \text{ \AA}$ ,  $b = 10.1920(1) \text{ \AA}$ ,  $c = 25.6079(3) \text{ \AA}$ ,  $V = 3548.81(6) \text{ \AA}^3$ ,  $Z = 4$ ]. Its layered open structure is attained by the presence of organic cations, water molecules and isolated sulfate tetrahedra between the inorganic lanthanum sulfate sheets. The decomposition of the two phases proceed through dehydration stages and lead to lanthanum oxide sulfates.

© 2003 Elsevier Inc. All rights reserved.

**Keywords:** Organically templated-lanthanum sulfate; Crystal structure determination; Amine; Open-framework structure; Thermal behavior

## 1. Introduction

There has been a fascinating interest in synthesizing non-alumino-silicate open-framework materials during the last decade. The work mainly focused on phosphates [1] and carboxylates (see, for example, Ref. [2]), but germanates [3] and arsenates [4] have also been involved in this research. Recently, new sulfates have been elaborated using organic templates. Cations involved in these compounds include transition metals (Cd [5], Fe [6]) and uranium [7]. An interesting feature of sulfate-based phases is the diversity of structure framework dimensionality. A representative illustration is obtained with lanthanum, which gives rise to a three-dimensional framework with piperazine [8] and layered structures with ethylenediamine [8,9]. Indeed, the ability of rare-earth elements to adopt a large range of coordination numbers [10] allows to obtain new topologies based on various polyhedra. In the course of investigations on hydrothermal synthesis of lanthanum sulfates in the presence of templating amines, two new compounds have been successfully prepared with the use of diethylenetriamine (dien),  $\text{La}(\text{C}_4\text{H}_{16}\text{N}_3)(\text{SO}_4)_3 \cdot \text{H}_2\text{O}$ ,

and 1,4-diazabicyclo[2,2,2]octane (dabco),  $\text{La}_2(\text{H}_2\text{O})_4(\text{C}_6\text{H}_{14}\text{N}_2)_2(\text{SO}_4)_5 \cdot 5\text{H}_2\text{O}$ . The present study deals with the crystal structure determination of these two compounds from single-crystal diffraction data and their thermal behavior investigated from powder diffraction data and thermal analyses.

## 2. Experimental

### 2.1. Synthesis of $\text{La}(\text{C}_4\text{H}_{16}\text{N}_3)(\text{SO}_4)_3 \cdot \text{H}_2\text{O}$

Lanthanum diethylenetriammonium sulfate, noted  $\text{La}(\text{dien})(\text{SO}_4)_3 \cdot \text{H}_2\text{O}$  hereafter, was prepared hydrothermally from  $\text{La}_2(\text{SO}_4)_3 \cdot 8\text{H}_2\text{O}$  (0.7 mmol), diethylenetriamine (dien) (2.8 mmol), concentrated sulfuric acid (0.5 mL) and distilled water (5 mL) in the molar ratio  $\text{La}:\text{dien}:\text{SO}_4:\text{H}_2\text{O} = 2:4:16:397$ . The homogeneous mixture was sealed in a 23 mL Teflon-lined acid digestion bomb (Parr) and heated at 423 K for 2 d. The resulting colorless crystals were obtained as a single phase.

### 2.2. Synthesis of $\text{La}_2(\text{H}_2\text{O})_4(\text{C}_6\text{H}_{14}\text{N}_2)_2(\text{SO}_4)_5 \cdot 5\text{H}_2\text{O}$

Lanthanum triethylenediammonium sulfate, noted  $\text{La}_2(\text{H}_2\text{O})_4(\text{dabco})_2(\text{SO}_4)_5 \cdot 5\text{H}_2\text{O}$  hereafter, was also

\*Corresponding author. Fax: +33-299-38-34-87.

E-mail address: [thierry.bataille@univ-rennes1.fr](mailto:thierry.bataille@univ-rennes1.fr) (T. Bataille).

obtained hydrothermally from  $\text{La}_2(\text{SO}_4)_3 \cdot 8\text{H}_2\text{O}$  (0.7 mmol), 1,4-diazabicyclo[2.2.2]octane (dabco) (2.1 mmol), concentrated sulfuric acid (0.31 mL) and distilled water (5 mL) in the molar ratio  $\text{La:dabco:SO}_4:\text{H}_2\text{O}=2:3:11:397$ . After the mixture was heated at 423 K for 2 d, colorless platy crystals were observed as a single phase.

### 2.3. Thermal analyses

Temperature Dependent X-ray Diffraction (TDXD) was performed with a powder diffractometer combining the curved-position-sensitive detector (CPS120) from INEL and a high temperature attachment from Rigaku. The detector was used in a semi-focusing geometry by reflection with the monochromatic  $\text{CuK}\alpha_1$  radiation, as described elsewhere [11]. In this geometry the flat sample is stationary. An angle of  $6^\circ$  between the incident beam and the surface of the sample was selected. Due to the stationary sample, preferred orientation effects can be strongly enhanced in case of micro-crystals present in the powder. In particular, intensities diffracted by  $hkl$  planes (and their higher orders) having Bragg angles in the vicinity of the incident angle of the beam can be significantly increased. This effect can appear suddenly if the position of the micro-crystals is slightly changed, due to the heating process (thermal expansion) or to phase transformations [11]. The thermal decomposition of the two compounds,  $\text{La}(\text{dien})(\text{SO}_4)_3 \cdot \text{H}_2\text{O}$  and  $\text{La}_2(\text{H}_2\text{O})_4(\text{dabco})_2(\text{SO}_4)_5 \cdot 5\text{H}_2\text{O}$ , were carried out under flowing air.

Thermogravimetric (TG) measurements were performed with a Rigaku Thermoflex instrument under flowing air, with a heating rate of  $6^\circ\text{C h}^{-1}$  and  $7^\circ\text{C h}^{-1}$  for the dien and the dabco compounds, respectively. The powdered samples, 99.97 mg for  $\text{La}(\text{dien})(\text{SO}_4)_3 \cdot \text{H}_2\text{O}$  and 79.75 mg for  $\text{La}_2(\text{H}_2\text{O})_4(\text{dabco})_2(\text{SO}_4)_5 \cdot 5\text{H}_2\text{O}$ , were spread evenly in a large platinum crucible to avoid mass effects.

### 2.4. Single-crystal diffraction data collection and structure determination

Small crystals of the two compounds were glued to a glass fiber mounted on a four-circle Nonius Kappa CCD area-detector diffractometer. Intensity data sets were collected using  $\text{MoK}\alpha$  radiation through the program COLLECT [12]. Correction for Lorentz-polarization effect, peak integration and background determination were carried out with the program DENZO [13]. Frame scaling and unit cell parameters refinement were performed with the program SCALEPACK [13]. Analytical absorption corrections were performed by modeling the crystal faces using NUMABS [14]. Crystallographic data are listed in Table 1.

#### 2.4.1. $\text{La}(\text{dien})(\text{SO}_4)_3 \cdot \text{H}_2\text{O}$

The structure was solved with the triclinic space group  $P-1$ . Lanthanum and sulfur atoms were located using the direct methods with the program SIR97 [15]. The oxygen atoms and the organic moiety were found from successive Fourier calculations using SHELXL-97 [16]. After several cycles of least-squares refinements, all H atoms were located by Fourier syntheses. C–H, O–H and central N–H distances were restrained to  $0.97(3)\text{Å}$ , while N–H bonds from terminal nitrogen atoms were restrained to  $0.89(3)\text{Å}$ .

#### 2.4.2. $\text{La}_2(\text{H}_2\text{O})_4(\text{dabco})_2(\text{SO}_4)_5 \cdot 5\text{H}_2\text{O}$

The structure analysis was initially carried out with the orthorhombic symmetry, space group  $Pbna$ , according to the automated search for space group available in WinGX [17]. A partial model, containing lanthanum atoms, bonded water oxygen atoms, sulfate groups and organic entities, was found by the direct methods program SIR97. Additional difference Fourier calculations revealed high electron density peaks separated by 1.25 and 1.75 Å, that could not correspond to the remaining five water oxygen atoms. Furthermore, systematic absence violations of many reflections ( $hk0$ ,  $h = 2n + 1$ ) with significant intensities were observed. Only space groups  $Pbnm$  and  $Pbn2_1$  were found in accordance with these reflections. The use of the centrosymmetric space group  $Pbnm$  in SIR97 did not reveal any consistent structure model. Consequently, the crystal structure was solved with the Patterson method (SHELXL-97) and the direct methods (SIR97) with space group  $Pbn2_1$ . Several Fourier calculations allowed to locate all non-hydrogen atoms. After transformation to the conventional setting  $Pna2_1$ , the H atoms were found from additional difference Fourier syntheses. The complete least-squares structure refinement was carried out with C–H and O–H distances restrained to  $0.97(2)\text{Å}$  and N–H distances to  $0.93(3)\text{Å}$ . The absolute structure was not determined, according to the value of the Flack parameter, i.e., 0.24(1). The examination of the atomic coordinates revealed that some pairs of similar atoms involved in the framework are related to each other through a center of symmetry. However, the coordinates of non-bonded light atoms, such as water oxygen atoms, cannot be transformed into a centrosymmetric space group. It is then assumed that the resulting structure is non-centrosymmetric. Similar cases involving heavy atoms in a centrosymmetric array have been discussed in literature (see, for example, Ref. [18]).

The results of the least-squares structure refinements for the two compounds are given in Table 1. Atomic coordinates and isotropic atomic displacement parameters of non-H atoms are given in Tables 2 and 3. Selected bond distances and angles, as well as probable hydrogen bonds, are listed in Tables 4 and 5 for

Table 1  
Crystallographic data for  $\text{La}(\text{dien})(\text{SO}_4)_3 \cdot \text{H}_2\text{O}$  and  $\text{La}_2(\text{H}_2\text{O})_4(\text{dabco})_2(\text{SO}_4)_5 \cdot 5\text{H}_2\text{O}$

	$\text{La}(\text{dien})(\text{SO}_4)_3 \cdot \text{H}_2\text{O}$	$\text{La}_2(\text{H}_2\text{O})_4(\text{dabco})_2(\text{SO}_4)_5 \cdot 5\text{H}_2\text{O}$
Empirical formula	$\text{C}_4\text{H}_{18}\text{LaN}_3\text{O}_{13}\text{S}_3$	$\text{C}_{12}\text{H}_{46}\text{La}_2\text{N}_4\text{O}_{29}\text{S}_5$
Formula weight ( $\text{g mol}^{-1}$ )	552.28	1148.65
Crystal system	Triclinic	Orthorhombic
Space group	$P-1$ (no. 2)	$Pna2_1$ (no. 33)
$a$ (Å)	8.2800(1)	13.5972(1)
$b$ (Å)	9.5755(2)	10.1920(1)
$c$ (Å)	10.4439(2)	25.6079(3)
$\alpha$ (deg)	105.689(1)	90
$\beta$ (deg)	102.844(1)	90
$\gamma$ (deg)	104.372(1)	90
$V$ (Å <sup>3</sup> )	734.12(2)	3548.81(6)
$Z$	2	4
$\rho_{\text{calc}}$ ( $\text{g cm}^{-3}$ )	2.494	2.150
Crystal size ( $\text{mm}^3$ )	$0.275 \times 0.200 \times 0.125$	$0.875 \times 0.125 \times 0.010$
$\lambda$ (MoK $\alpha$ ) (Å)	0.71073	0.71073
$\mu$ ( $\text{mm}^{-1}$ )	3.415	2.778
$\theta$ range (deg)	2.67–34.97	2.91–32.03
Index ranges	$-13 \leq h \leq 13$ $-15 \leq k \leq 15$ $-13 \leq l \leq 16$	$-20 \leq h \leq 12$ $-15 \leq k \leq 14$ $-38 \leq l \leq 38$
Unique data	6315	12000
Observed data [ $I > 2\sigma(I)$ ]	5491	9395
$R_{\text{int}}$	0.0421	0.0564
Refinement method	Full matrix least-squares on $ F^2 $	
$R_1$ [ $I > 2\sigma(I)$ ]	0.0270	0.0355
$R_1$ (all data)	0.0329	0.0530
$wR_2$ [ $I > 2\sigma(I)$ ]	0.0618	0.0756
$wR_2$ (all data)	0.0659	0.0829
GoF	1.106	1.019
No. of variables	293	609
No. of restraints	18	64
Largest difference map peak and hole ( $\text{e} \text{Å}^{-3}$ )	2.08 and $-1.33$	1.39 and $-1.55$

$\text{La}(\text{dien})(\text{SO}_4)_3 \cdot \text{H}_2\text{O}$  and Tables 6 and 7 for  $\text{La}_2(\text{H}_2\text{O})_4(\text{dabco})_2(\text{SO}_4)_5 \cdot 5\text{H}_2\text{O}$ .

### 3. Results

#### 3.1. Description of the structures

##### 3.1.1. $\text{La}(\text{dien})(\text{SO}_4)_3 \cdot \text{H}_2\text{O}$

The one-dimensional crystal structure consists of strictly linear anionic chains  $[\text{La}(\text{SO}_4)_3]_{\infty}^{3-}$  running along the  $a$ -axis, between which are located dien<sup>3+</sup> cations and water molecules (Fig. 1). Within a chain, the lanthanum atoms, lying in special positions (0,0,0) and (1/2,0,0) of space group  $P-1$ , are linked together in 12-fold coordination with the sulfate anions arranged in helical manner along the  $a$ -axis. Each  $\text{SO}_4$  tetrahedron is connected through two adjacent edges with La atoms, so that one oxygen atom (O12, O21 and O32) is shared by La1 and La2, one oxygen atom (O13, O24 and O31) is bonded to La1 and one atom (O11, O22 and O33) is bonded to La2, while the fourth O atom (O14, O23 and

O34) lies out of the chain (Fig. 2). The La–O distances range between 2.588(1) and 2.842(2) Å (Table 4), with a mean distance 2.709(1) Å, in agreement with the value 2.685 Å calculated from the bond valence program VALENCE [19] for a 12-fold oxygen-coordinated lanthanum atom. The diethylenetriamine groups lie between the chains so that one dien<sup>3+</sup> forms strong hydrogen bonds with sulfate oxygen atoms of three chains. The water molecule is H bond acceptor from the terminal nitrogen atom N1 and H bond donor bonded to two sulfate O atoms. Within the sulfate groups, the S–O bond lengths are comprised between 1.446(1) and 1.510(1) Å [average value 1.478(1) Å] and the O–S–O angles range from 105.02(8)° to 112.91(9)° [average value 109.41(9)°]. These values are in agreement with those commonly observed in metal sulfates [8,20]. It should be noted that the shortest S–O bond lengths are observed for O atoms non-bonded to La atoms, i.e., 1.452(2) Å for S1–O14, 1.446(1) Å for S2–O23 and 1.453(2) Å for S3–O34. In the same way, the O atoms connected to two La atoms involve the longest S–O distances, i.e., 1.510(1) Å for S1–O12, 1.508(1) Å for

Table 2

Selected atomic coordinates and isotropic atomic displacement parameters ( $\text{\AA}^2$ ) for  $\text{La}(\text{C}_6\text{H}_{16}\text{N}_3)(\text{SO}_4)_3 \cdot \text{H}_2\text{O}$ 

Atom	$x/a$	$y/b$	$z/c$	$U_{\text{eq}}^a$
La1	1	0	0	0.01206(5)
La2	1/2	0	0	0.01133(5)
S1	0.85887(5)	0.14018(5)	0.27393(4)	0.01239(8)
O11	0.6860(2)	0.0404(2)	0.2683(2)	0.0182(3)
O12	0.8269(2)	0.1678(2)	0.1362(1)	0.0162(2)
O13	0.9890(2)	0.0603(2)	0.2758(2)	0.0220(3)
O14	0.9175(2)	0.2838(2)	0.3904(2)	0.0248(3)
S2	1.25172(6)	-0.16277(5)	0.16601(5)	0.01240(8)
O21	1.2890(2)	-0.0028(2)	0.1597(1)	0.0161(2)
O22	0.3689(2)	-0.2272(2)	0.0987(1)	0.0169(3)
O23	1.2837(2)	-0.1583(2)	0.3092(2)	0.0235(3)
O24	1.0656(2)	-0.2455(2)	0.0824(2)	0.0214(3)
S3	1.35887(6)	0.29591(5)	0.09917(5)	0.01258(8)
O31	1.2292(2)	0.2820(2)	0.1756(2)	0.0204(3)
O32	1.2825(2)	0.1564(2)	-0.0317(1)	0.0150(2)
O33	0.5250(2)	0.2852(2)	0.1761(2)	0.0220(3)
O34	1.3870(2)	0.4343(2)	0.0629(2)	0.0246(3)
N1	0.4776(3)	0.7849(3)	0.5575(2)	0.0302(4)
C2	0.6155(3)	0.8097(3)	0.4891(2)	0.0238(4)
C3	0.5618(3)	0.6782(2)	0.3523(2)	0.0165(3)
N4	0.6638(2)	0.7194(2)	0.2590(2)	0.0177(3)
C5	0.8536(2)	0.7316(2)	0.3061(2)	0.0181(3)
C6	0.8844(3)	0.5797(2)	0.2882(2)	0.0189(4)
N7	0.8593(3)	0.4922(2)	0.1399(2)	0.0264(4)
OW	0.2530(2)	0.4798(2)	0.4289(2)	0.0333(4)

<sup>a</sup>  $U_{\text{eq}}$  is defined as one-third of the trace of the orthogonalized  $U_{ij}$  tensor.

S2–O21 and 1.504(1) Å for S3–O32. This is due to the fact that the strengths of the La–O bonds are stronger than the other bonds formed with O atoms. Indeed, the mean valence of the bonds between La and O atoms sharing two lanthanum atoms is 0.284, while for the sulfate O atoms which are only hydrogen bonded, the valence of the H...O bond is about 0.2 [21]. It also implies that the longer the S–O bond, the shorter the La–O bond and inversely. This result can be generalized to all bonds involving oxygen atoms, considering that the sum of the bond valence around the O atom is equal to the charge 2– of the atom (see, for instance, the bond valence sum rule in Ref. [22]).

A few organically templated metal sulfates with one-dimensional structures have been reported recently. Linear uranyl sulfates, namely USO-1 [23], USO-3 [24], USO-6, USO-7, USO-9 [7] and USO-22 [25], are all built from  $\text{UO}_7$  polyhedra, which are connected via the  $\text{SO}_4$  tetrahedra and contain also non-sulfate O atoms. In the recently reported cadmium sulfates [5,26], the metal coordination sphere contains halogen atoms, i.e., Fe surrounded by fluorine atoms in iron sulfates [6] and V polyhedra involving either OH groups or  $\text{H}_2\text{O}$  molecules in vanadyl sulfates [27]. The structure of  $(\text{NH}_4)_5[\text{La}(\text{SO}_4)_4]$  is also built from lanthanum atoms connected by sulfate groups only, but the chains adopt a

Table 3

Selected atomic coordinates and isotropic atomic displacement parameters ( $\text{\AA}^2$ ) for  $\text{La}_2(\text{H}_2\text{O})_4(\text{C}_6\text{H}_{14}\text{N}_2)_2(\text{SO}_4)_5 \cdot 5\text{H}_2\text{O}$ 

Atom	$x/a$	$y/b$	$z/c$	$U_{\text{eq}}^a$
La1	0.21979(2)	0.23667(3)	-0.139480(8)	0.01232(8)
La2	0.21594(2)	0.73594(3)	0.012072(8)	0.01252(8)
S1	0.22653(8)	0.4826(2)	-0.06093(8)	0.0147(4)
O11	0.3118(2)	0.4203(4)	-0.0863(2)	0.024(1)
O12	0.1399(2)	0.4036(4)	-0.0757(2)	0.019(1)
O13	0.2153(2)	0.6199(5)	-0.0780(2)	0.019(1)
O14	0.2378(2)	0.4894(4)	-0.0031(2)	0.020(1)
S2	-0.00859(9)	0.2135(2)	-0.16520(7)	0.0177(3)
O21	0.0430(2)	0.1525(4)	-0.1208(2)	0.027(1)
O22	0.0644(2)	0.3044(4)	-0.1888(2)	0.0216(9)
O23	0.4045(2)	0.2136(4)	-0.1467(2)	0.022(1)
O24	-0.0384(2)	0.1129(4)	-0.2026(2)	0.029(1)
S3	-0.01391(9)	0.7166(2)	0.03550(7)	0.0163(3)
O31	0.4008(2)	0.7078(4)	0.0175(2)	0.022(1)
O32	-0.0478(2)	0.6152(4)	0.0729(2)	0.032(1)
O33	0.0393(2)	0.6536(4)	-0.0090(2)	0.021(1)
O34	0.0578(2)	0.8050(4)	0.0607(2)	0.022(1)
S4	0.22557(8)	-0.0181(2)	-0.06651(8)	0.0142(4)
O41	0.2141(2)	0.1202(5)	-0.0485(2)	0.019(1)
O42	0.1378(2)	-0.0983(4)	-0.0529(2)	0.019(1)
O43	0.2396(2)	-0.0122(4)	-0.1234(2)	0.021(1)
O44	0.3098(2)	-0.0819(4)	-0.0411(2)	0.024(1)
S5	0.2566(1)	0.30871(9)	-0.8171(1)	0.0256(2)
O51	0.1742(4)	0.2337(5)	-0.7953(3)	0.048(2)
O52	0.3353(3)	0.2165(4)	-0.8320(3)	0.040(1)
O53	0.2935(3)	0.4007(5)	-0.7797(2)	0.060(2)
O54	0.2248(3)	0.3714(5)	-0.8664(2)	0.057(2)
O91	0.2519(2)	0.9153(5)	0.0771(2)	0.029(1)
O92	0.2277(3)	0.6195(6)	0.0979(3)	0.038(1)
O93	0.2619(3)	0.4145(5)	-0.2023(2)	0.031(1)
O94	0.2386(3)	0.1216(5)	-0.2247(2)	0.031(1)
N1	0.9705(3)	0.2831(6)	-0.6274(3)	0.026(2)
C11	0.9120(4)	0.2411(8)	-0.6732(4)	0.036(2)
C12	1.0119(4)	0.4170(6)	-0.6365(4)	0.030(2)
C13	1.0527(4)	0.1842(8)	-0.6174(3)	0.030(2)
N2	1.0801(3)	0.2763(5)	-0.7048(3)	0.022(1)
C21	0.9839(4)	0.2116(8)	-0.7177(3)	0.027(2)
C22	1.0605(4)	0.4165(6)	-0.6892(3)	0.026(2)
C23	1.1298(4)	0.2075(7)	-0.6603(3)	0.029(2)
N3	0.5319(3)	0.2801(6)	-0.0019(3)	0.025(2)
C31	0.4517(4)	0.1850(9)	-0.0124(3)	0.030(2)
C32	0.4883(4)	0.4124(7)	0.0088(4)	0.034(2)
C33	0.5917(4)	0.2373(7)	0.0446(4)	0.030(2)
N4	0.4240(3)	0.2678(5)	0.0759(3)	0.021(1)
C41	0.3759(4)	0.1996(7)	0.0304(3)	0.029(2)
C42	0.4388(4)	0.4071(7)	0.0627(3)	0.025(1)
C43	0.5208(4)	0.2019(8)	0.0878(3)	0.033(2)
O95	0.1410(4)	0.4995(6)	-0.2741(3)	0.083(2)
O96	0.0436(2)	0.0664(4)	-0.3011(2)	0.0425(9)
O97	0.0142(4)	0.3298(5)	-0.3234(2)	0.064(1)
O98	0.3176(4)	0.2382(4)	-0.3096(2)	0.049(1)
O99	0.3641(3)	0.5003(5)	-0.3436(2)	0.055(2)

<sup>a</sup>  $U_{\text{eq}}$  is defined as one-third of the trace of the orthogonalized  $U_{ij}$  tensor.

zigzag conformation [28]. It is noteworthy that, in the structure of  $\text{La}(\text{dien})(\text{SO}_4)_3 \cdot \text{H}_2\text{O}$ , the La atoms propagate along the  $a$ -axis in a strictly linear manner, and that they are surrounded by sulfate oxygen atoms only.

Table 4  
Selected bond distances (Å) and angles (deg) in La(dien)(SO<sub>4</sub>)<sub>3</sub>·H<sub>2</sub>O

Within La polyhedra			
La1–O12, O12 <sup>I</sup>	2.734(1)	La2–O11, O11 <sup>II</sup>	2.752(1)
La1–O13, O13 <sup>I</sup>	2.808(2)	La2–O12, O12 <sup>II</sup>	2.613(1)
La1–O21, O21 <sup>I</sup>	2.606(1)	La2–O21 <sup>I</sup> , O21 <sup>III</sup>	2.671(1)
La1–O24, O24 <sup>I</sup>	2.842(2)	La2–O22, O22 <sup>II</sup>	2.740(1)
La1–O31, O31 <sup>I</sup>	2.736(2)	La2–O32 <sup>I</sup> , O32 <sup>III</sup>	2.635(1)
La1–O32, O32 <sup>I</sup>	2.588(1)	La2–O33, O33 <sup>II</sup>	2.778(2)
Within diethylenetriammonium ions			
N1–C2	1.480(3)	N1–C2–C3	109.2(2)
C2–C3	1.513(3)	C2–C3–N4	111.3(2)
C3–N4	1.492(2)	C3–N4–C5	114.9(2)
N4–C5	1.503(2)	N4–C5–C6	114.4(2)
C5–C6	1.509(3)	C5–C6–N7	112.6(2)
C6–N7	1.487(3)		

Symmetry codes: I, 2 – x, –y, –z; II, 1 – x, –y, –z; III, –1 + x, y, z.

Table 5  
Possible hydrogen bonds in La(dien)(SO<sub>4</sub>)<sub>3</sub>·H<sub>2</sub>O

D–H...A	d(D–H) (Å)	d(H...A) (Å)	d(D...A) (Å)	∠D–H...A (deg)
N1–H11...OW	0.89(3)	1.93(3)	2.804(3)	165(4)
N1–H12...O21 <sup>I</sup>	0.91(3)	2.16(4)	2.990(3)	151(5)
N1–H12...O33 <sup>II</sup>	0.91(3)	2.38(4)	3.037(3)	129(4)
N1–H13...O23 <sup>III</sup>	0.91(3)	2.27(4)	2.990(3)	137(4)
N4–H41...O34 <sup>IV</sup>	0.95(2)	2.16(3)	2.946(2)	139(2)
N4–H42...O11 <sup>V</sup>	0.94(2)	2.09(2)	3.008(2)	164(3)
N4–H42...O22 <sup>V</sup>	0.94(2)	2.39(3)	2.880(2)	113(2)
N4–H42...O32 <sup>VI</sup>	0.94(2)	2.49(3)	2.997(2)	114(2)
N7–H71...O24 <sup>V</sup>	0.92(2)	2.10(3)	2.955(3)	154(3)
N7–H72...O34 <sup>VI</sup>	0.91(2)	2.27(3)	2.957(3)	132(3)
N7–H72...O22 <sup>VII</sup>	0.91(2)	2.32(4)	2.886(2)	120(3)
N7–H73...O12	0.94(2)	2.20(3)	3.039(2)	148(3)
N7–H73...O24 <sup>VIII</sup>	0.94(2)	2.51(4)	3.124(2)	123(3)
OW–HW1...O14 <sup>IV</sup>	0.88(2)	1.96(3)	2.812(2)	163(3)
OW–HW2...O31 <sup>IV</sup>	0.91(2)	1.84(2)	2.738(2)	171(3)

Symmetry codes: I, 2 – x, 1 – y, 1 – z; II, 1 – x, 1 – y, 1 – z; III, –1 + x, 1 + y, z; IV, –1 + x, y, z; V, x, 1 + y, z; VI, 2 – x, 1 – y, –z; VII, 1 – x, –y, –z; VIII, 2 – x, –y, –z; IX, 1 + x, y, z.

### 3.1.2. La<sub>2</sub>(H<sub>2</sub>O)<sub>4</sub>(dabco)<sub>2</sub>(SO<sub>4</sub>)<sub>5</sub>·5H<sub>2</sub>O

The two-dimensional crystal structure consists of corrugated layers of global formula [La<sub>2</sub>(H<sub>2</sub>O)<sub>4</sub>(SO<sub>4</sub>)<sub>4</sub>]<sup>2–</sup><sub>∞</sub>, perpendicular to the *c*-axis, between which are located isolated SO<sub>4</sub><sup>2–</sup> anions. Fig. 3 shows that such arrangement of sulfate tetrahedra leads to side-open channels running along the *a*-axis. The charge-compensating dabco<sup>2+</sup> cations are situated in cavities arising from the inorganic corrugated sheets, while the five non-bonded water molecules are located in the interlayer space together with isolated SO<sub>4</sub><sup>2–</sup> groups. It is interesting to note that the water molecules connected to the La atoms point out towards the tunnels containing the non-bonded water molecules, so that the vacant spaces can be considered as either hydrophilic or hydrophobic channels. The lanthanum atoms are nine-fold coordi-

Table 6  
Selected bond distances (Å) and angles (deg) in La<sub>2</sub>(H<sub>2</sub>O)<sub>4</sub>(dabco)<sub>2</sub>(SO<sub>4</sub>)<sub>5</sub>·5H<sub>2</sub>O

Within La polyhedra			
La1–O11	2.631(4)	La2–O13	2.593(6)
La1–O12	2.597(4)	La2–O14	2.560(4)
La1–O21	2.596(3)	La2–O31	2.534(3)
La1–O22	2.557(4)	La2–O33	2.600(3)
La1–O23	2.530(3)	La2–O34	2.583(4)
La1–O41	2.616(6)	La2–O42 <sup>I</sup>	2.598(4)
La1–O43	2.584(4)	La2–O44 <sup>I</sup>	2.633(4)
La1–O93	2.490(5)	La2–O91	2.521(5)
La1–O94	2.491(6)	La2–O92	2.503(6)
Within dabco cations			
N1–C11	1.48(1)	N3–C31	1.484(9)
N1–C12	1.494(8)	N3–C32	1.498(8)
N1–C13	1.527(8)	N3–C33	1.51(1)
N2–C21	1.502(8)	N4–C41	1.51(1)
N2–C22	1.507(8)	N4–C42	1.474(8)
N2–C23	1.498(9)	N4–C43	1.508(8)
C11–C21	1.53(1)	C31–C41	1.512(9)
C12–C22	1.50(1)	C32–C42	1.54(1)
C13–C23	1.54(1)	C33–C43	1.51(1)
C11–N1–C12	110.1(7)	C31–N3–C32	109.2(4)
C11–N1–C13	109.6(6)	C31–N3–C33	110.5(6)
C12–N1–C13	110.7(4)	C32–N3–C33	109.2(6)
N1–C11–C21	107.7(4)	N3–C31–C41	107.8(6)
N1–C12–C22	107.6(6)	N3–C32–C42	107.9(6)
N1–C13–C23	106.1(5)	N3–C33–C43	107.7(4)
C21–N2–C22	108.7(5)	C41–N4–C42	109.1(6)
C21–N2–C23	110.8(6)	C41–N4–C43	109.3(5)
C22–N2–C23	108.8(6)	C42–N4–C43	110.9(5)
N2–C21–C11	107.8(6)	N4–C41–C31	108.1(4)
N2–C22–C12	108.5(5)	N4–C42–C32	107.4(5)
N2–C23–C13	107.9(4)	N4–C43–C33	107.5(6)

Symmetry codes: I, x, 1 + y, z.

nated to two water oxygen atoms and seven sulfate oxygen atoms. The La–O distances fall into the range 2.490(5)–2.633(4) Å (Table 6), mean value 2.568(4) Å, in agreement with the length calculated from the bond valence model, i.e., 2.579 Å. As explained above for La(dien)(SO<sub>4</sub>)<sub>3</sub>·H<sub>2</sub>O, the shortest distances are observed between the lanthanum atoms and the water oxygen atoms. The SiO<sub>4</sub> and S4O<sub>4</sub> tetrahedra are both bidentate towards La1 and La2, so that they ensure the propagation of a layer along the *b*-axis with the sequence [–S4O<sub>4</sub>–La1–SiO<sub>4</sub>–La2–] (Fig. 4a). Such μ-4 bridging mode of the SO<sub>4</sub><sup>2–</sup> anion is not frequently observed, as discussed elsewhere [29]. The S2O<sub>4</sub> and S3O<sub>4</sub> groups are both bidentate and monodentate to two La1 and two La2, respectively. The propagation of a layer is then ensured along the *a*-axis by two adjacent chains with the sequences [–La1–S2O<sub>4</sub>–La1–S2O<sub>4</sub>–] and [–La2–S3O<sub>4</sub>–La2–S3O<sub>4</sub>–]. The fourth O atoms of the S2O<sub>4</sub> and S3O<sub>4</sub> tetrahedra (O24 and O32) lie out of the layer in the direction of the hydrophilic channels. The fifth sulfate group, S5O<sub>4</sub>, is located at the middle of

Table 7  
Possible hydrogen bonds in  $\text{La}_2(\text{H}_2\text{O})_4(\text{dabco})_2(\text{SO}_4)_5 \cdot 5\text{H}_2\text{O}$

D–H...A	$d(\text{D–H})$ (Å)	$d(\text{H...A})$ (Å)	$d(\text{D...A})$ (Å)	$\angle \text{D–H...A}$ (deg)
O91–H911...O99 <sup>I</sup>	0.94(2)	1.83(3)	2.712(7)	154(5)
O91–H912...O32 <sup>II</sup>	0.95(2)	1.99(3)	2.744(5)	135(4)
O92–H921...O54 <sup>III</sup>	0.97(2)	1.78(3)	2.689(8)	155(5)
O92–H922...O98 <sup>I</sup>	0.96(2)	1.78(2)	2.730(8)	172(6)
O93–H931...O95	0.97(2)	1.66(2)	2.615(7)	166(5)
O93–H932...O24 <sup>IV</sup>	0.96(2)	1.86(3)	2.729(5)	148(4)
O94–H941...O98	0.96(2)	1.74(2)	2.700(7)	178(5)
O94–H942...O53 <sup>V</sup>	0.96(2)	1.78(3)	2.692(8)	158(5)
O95–H951...O97	0.94(2)	1.97(4)	2.749(7)	138(5)
O95–H952...O52 <sup>I</sup>	0.94(2)	1.75(2)	2.681(8)	174(8)
O96–H961...O24	0.96(2)	1.90(3)	2.799(6)	154(5)
O96–H962...O53 <sup>V</sup>	0.94(2)	2.05(4)	2.839(6)	140(5)
O97–H971...O96	0.97(2)	1.85(4)	2.773(7)	157(7)
O97–H972...O32 <sup>VI</sup>	0.96(2)	1.80(2)	2.750(7)	170(7)
O98–H981...O97 <sup>IV</sup>	0.97(2)	1.91(4)	2.785(7)	149(6)
O98–H982...O99	0.98(2)	2.05(4)	2.880(7)	141(5)
O99–H991...O51 <sup>I</sup>	0.94(2)	1.83(3)	2.732(7)	159(7)
O99–H992...O96 <sup>IV</sup>	0.93(2)	1.83(2)	2.758(6)	169(6)
N1–H1...O42 <sup>VII</sup>	0.90(3)	2.34(5)	3.059(8)	136(5)
N1–H1...O13 <sup>VIII</sup>	0.90(3)	2.35(5)	2.993(6)	128(5)
N1–H1...O33 <sup>VIII</sup>	0.90(3)	2.44(6)	3.104(9)	131(5)
N2–H2...O51	0.95(3)	1.79(4)	2.683(9)	155(5)
N3–H3...O41 <sup>IV</sup>	0.94(3)	2.16(5)	2.931(6)	138(5)
N3–H3...O21 <sup>IV</sup>	0.94(3)	2.38(5)	3.124(9)	135(5)
N3–H3...O12 <sup>IV</sup>	0.94(3)	2.50(6)	3.038(8)	116(4)
N4–H4...O52 <sup>III</sup>	0.94(3)	1.77(3)	2.700(9)	173(5)

Symmetry codes: I,  $1/2 - x, 1/2 + y, 1/2 + z$ ; II,  $1/2 + x, 3/2 - y, z$ ; III,  $x, y, 1 + z$ ; IV,  $1/2 + x, 1/2 - y, z$ ; V,  $1/2 - x, -1/2 + y, 1/2 + z$ ; VI,  $-x, 1 - y, -1/2 + z$ ; VII,  $1 - x, -y, -1/2 + z$ ; VIII,  $1 - x, 1 - y, -1/2 + z$ ; IX,  $1 + x, y, z$ .

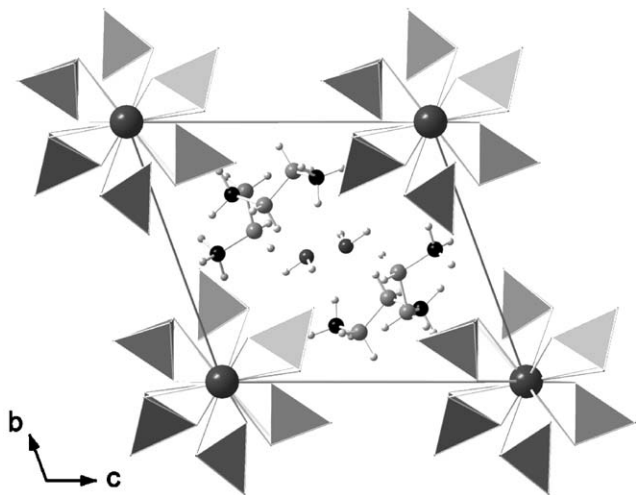


Fig. 1. Projection of the structure of  $\text{La}(\text{dien})(\text{SO}_4)_3 \cdot \text{H}_2\text{O}$  along the  $a$ -axis.

the interlayer space and is retained to the structure via a complex hydrogen bond scheme including water molecules and  $\text{dabco}^{2+}$  cations, as shown in Figs. 4b–d. The geometric parameters within the  $\text{dabco}^{2+}$  cations are in good agreement with that commonly observed in the literature (see Table 6 and Ref. [30]).

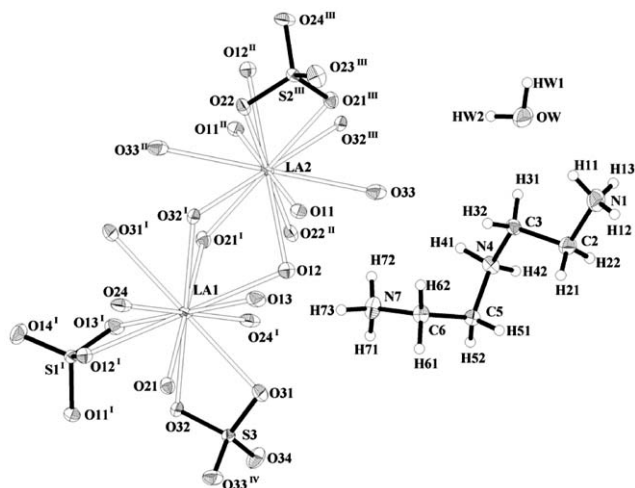


Fig. 2. Displacement ellipsoid plot of  $\text{La}(\text{dien})(\text{SO}_4)_3 \cdot \text{H}_2\text{O}$ , showing the environment of the La atoms, the amine group and the water molecule. Ellipsoids are drawn at the 50% probability level.

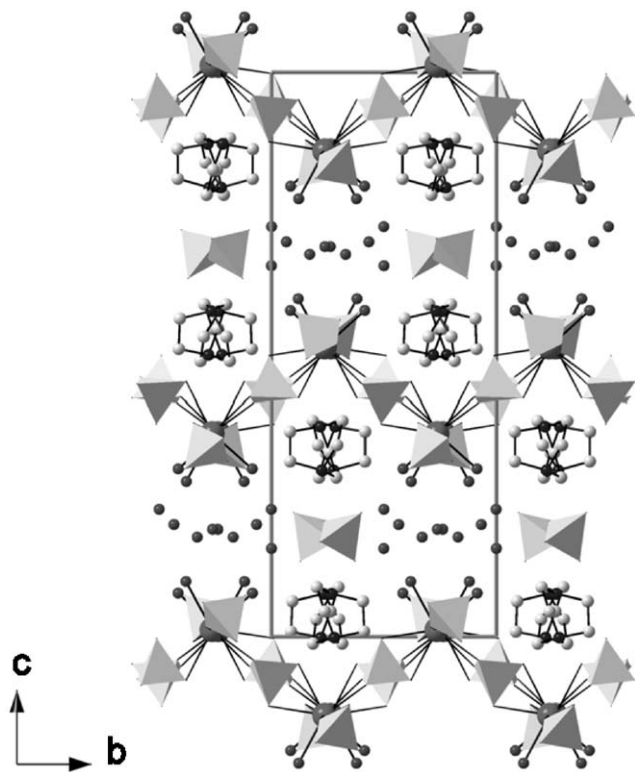


Fig. 3. Projection of the structure of  $\text{La}_2(\text{H}_2\text{O})_4(\text{dabco})_2(\text{SO}_4)_5 \cdot 5\text{H}_2\text{O}$  along the  $a$ -axis.

It is interesting to discuss this layered structure with respect to other known structures reported for sulfate-based rare-earth compounds, such as  $\text{La}_2(\text{H}_2\text{O})_2(\text{en})_3(\text{SO}_4)_6 \cdot 4\text{H}_2\text{O}$  [8] and  $\text{La}_2(\text{H}_2\text{O})_4(\text{en})(\text{SO}_4)_4 \cdot 2\text{H}_2\text{O}$  [9] (where en stands for ethylenediamine),  $\beta\text{-(NH}_4\text{)La}(\text{SO}_4)_2$  [31],  $(\text{N}_2\text{H}_5)\text{Nd}(\text{H}_2\text{O})(\text{SO}_4)_2$  [32]. Indeed, the inorganic corrugated sheets are similar in the compound described here and in  $\text{La}_2(\text{H}_2\text{O})_2(\text{en})_3(\text{SO}_4)_6 \cdot 4\text{H}_2\text{O}$  and

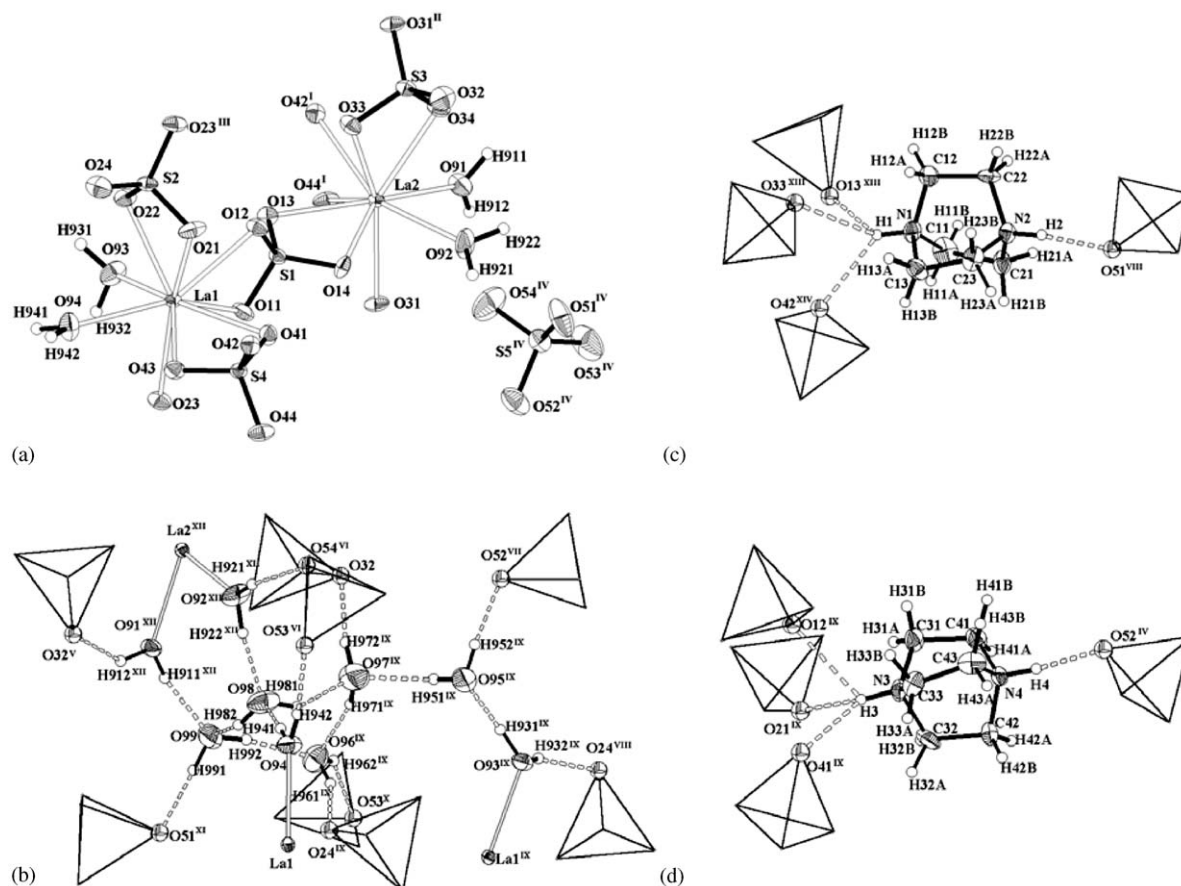


Fig. 4. Displacement ellipsoid plots of  $\text{La}_2(\text{H}_2\text{O})_4(\text{dabco})_2(\text{SO}_4)_5 \cdot 5\text{H}_2\text{O}$ , showing (a) the environment of La atoms, (b) the hydrogen bonding scheme of the water molecules, (c) and (d) the hydrogen bonds formed with the  $\text{dabco}^{2+}$  cations. Ellipsoids are drawn at the 50% probability level.

$\text{La}_2(\text{H}_2\text{O})_4(\text{en})(\text{SO}_4)_4 \cdot 2\text{H}_2\text{O}$ . The distance between the middle planes of the sheets is 12.80 Å (closest La atoms distance, 8.92 Å, farthest La atoms distance, 16.68 Å). The shortest O–O distance between two adjacent layers is 4.566(9) Å between O92 and O94, due to the presence of the intercalated  $\text{SO}_4^{2-}$  groups between the layers. This result contrasts with those observed in other reported lanthanide-based layered sulfates, for which the shortest O–O distance is about 3.10 Å in the ammonium and hydrazinium compounds and 3.02 Å in  $\text{La}_2(\text{H}_2\text{O})_2(\text{en})_3(\text{SO}_4)_6 \cdot 4\text{H}_2\text{O}$ .

### 3.2. Thermal decomposition

#### 3.2.1. $\text{La}(\text{dien})(\text{SO}_4)_3 \cdot \text{H}_2\text{O}$

The TG analysis (Fig. 5) shows that the dehydration starts at 70°C and corresponds to the departure of the single water molecule located between the chain (observed and calculated weight losses 3.3%). The TDXD plot was not informative, since it shows only the dehydration of the precursor into a poorly crystalline phase. The anhydrous compound, pointed out with the first plateau observed on the TG curve, is stable

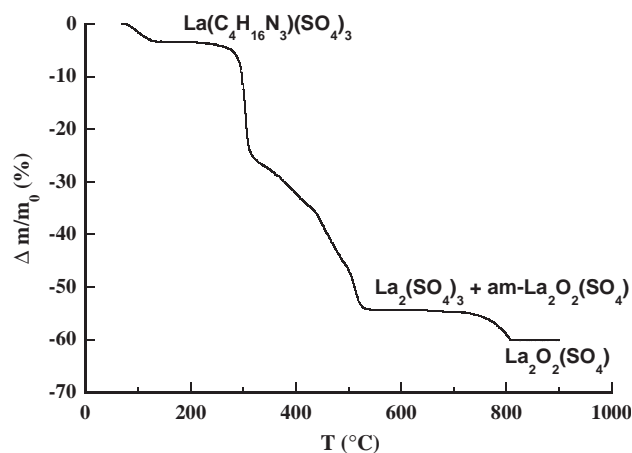


Fig. 5. TG curve for the decomposition of  $\text{La}(\text{dien})(\text{SO}_4)_3 \cdot \text{H}_2\text{O}$  in air ( $6^\circ\text{C h}^{-1}$ ).

between 135°C and 200°C. Its decomposition starts slowly at 200°C and becomes faster at 275°C, in agreement with the decomposition of the amine entity. The second plateau is observed in the temperature range 534–720°C. It corresponds to a compound with the

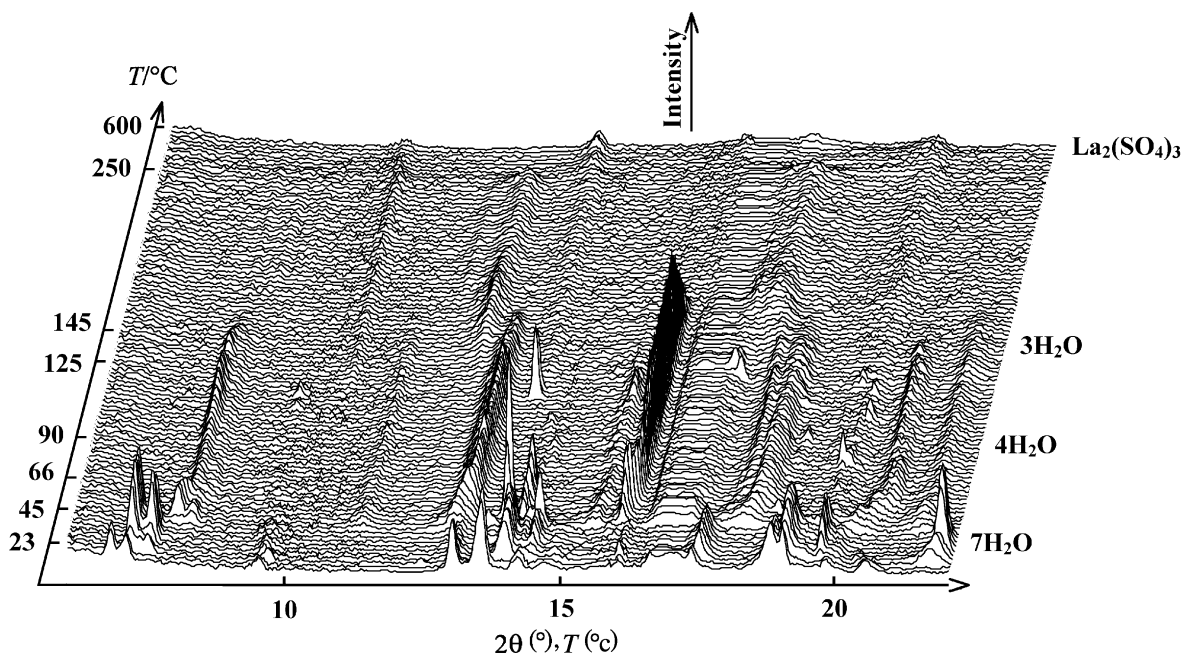


Fig. 6. TDXD plot for the thermal decomposition of  $\text{La}_2(\text{H}_2\text{O})_4(\text{dabco})_2(\text{SO}_4)_5 \cdot 5\text{H}_2\text{O}$  in air ( $2^\circ\text{C h}^{-1}$  from  $18^\circ\text{C}$  to  $250^\circ\text{C}$ ,  $30^\circ\text{C h}^{-1}$  from  $250^\circ\text{C}$  to  $600^\circ\text{C}$ , counting time of 4800 s per pattern).

global formula “ $\text{La}_2\text{O}(\text{SO}_4)_2$ ”, according to the observed weight loss of 54.2% (theoretical weight loss, 55.8%). In situ powder diffraction data analysis revealed that, at  $600^\circ\text{C}$ , the diffraction lines of this material correspond to those of  $\text{La}_2(\text{SO}_4)_3$  (ICDD PDF No. 39-0301) [33]. Consequently, it can be suggested that the product with a global formula “ $\text{La}_2\text{O}(\text{SO}_4)_2$ ” is in fact a mixture of crystalline  $\text{La}_2(\text{SO}_4)_3$  and  $\text{La}_2\text{O}_2\text{SO}_4$  amorphous to X-rays. The end of its decomposition is marked again by a plateau at  $815^\circ\text{C}$  corresponding to the partial decomposition of  $\text{La}_2(\text{SO}_4)_3$  into  $\text{La}_2\text{O}_2\text{SO}_4$  (observed weight loss, 60.0%, theoretical weight loss for  $\text{La}_2\text{O}_2\text{SO}_4$ , 63.0%).

### 3.2.2. $\text{La}_2(\text{H}_2\text{O})_4(\text{dabco})_2(\text{SO}_4)_5 \cdot 5\text{H}_2\text{O}$

The dehydration process is revealed by the TDXD plot (Fig. 6) and the TG curve (Fig. 7). Fig. 6 shows that several changes in the diffraction patterns are observed between room temperature and  $145^\circ\text{C}$ . These modifications are related to four weight losses, in agreement with the release of two water molecules between  $20^\circ\text{C}$  and  $40^\circ\text{C}$ , three water molecules between  $45^\circ\text{C}$  and  $90^\circ\text{C}$ , one  $\text{H}_2\text{O}$  molecule between  $125^\circ\text{C}$  and  $145^\circ\text{C}$  and the three last water molecules between  $145^\circ\text{C}$  and  $260^\circ\text{C}$  (observed and theoretical weight losses, 13.8% and 14.1%). Though the three-dimensional plot reveals that the successive hydrates are crystalline, additional in situ X-ray data collections did not allow to index the corresponding patterns, mainly due to significant diffraction line broadening which occurs during the decomposition process and severe line overlaps arising

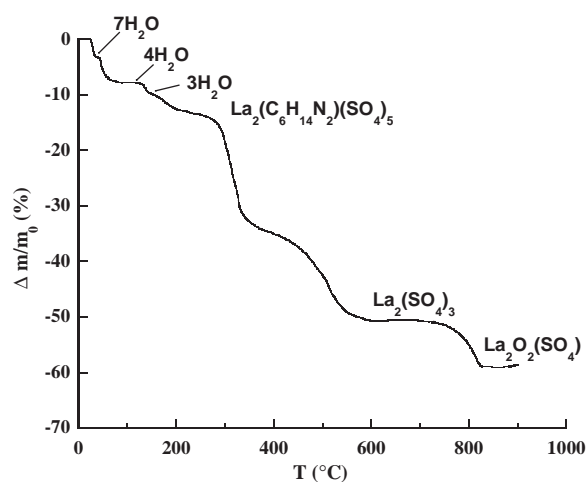


Fig. 7. TG curve for the decomposition of  $\text{La}_2(\text{H}_2\text{O})_4(\text{dabco})_2(\text{SO}_4)_5 \cdot 5\text{H}_2\text{O}$  in air ( $7^\circ\text{C h}^{-1}$ ). The water molecule content in the compounds is indicated for each dehydration stage.

from high cell volumes, as suggested from that of the precursor ( $3549 \text{ \AA}^3$ ). Nevertheless, it is worth noting that the release of three water molecules between  $45^\circ\text{C}$  and  $90^\circ\text{C}$  is accompanied by a significant shift of some diffraction lines to the higher angles, which may be an indication of a smaller interlayer spacing, and the disappearance of some reflections, as pointed out in the TDXD plot between  $45^\circ\text{C}$  and  $66^\circ\text{C}$ . As depicted in the TG curve, anhydrous lanthanum dabco sulfate is not stable and decomposes slowly from  $270^\circ\text{C}$ . The weight loss at the inflection is 33.9%, which can be interpreted



by the decomposition of the amine group. The decomposition of some sulfate entities leads to  $\text{La}_2(\text{SO}_4)_3$  (observed and theoretical weight losses, 50.6%), also identified in the TDXD plot (ICDD PDF No. 39-0301). The final plateau, reached at 825°C, corresponds to a weight loss of 59.0%. According to the weight loss 64.5% calculated for  $\text{La}_2\text{O}_2\text{SO}_4$ , it is assumed that  $\text{La}_2(\text{SO}_4)_3$  only partially decomposes.

#### 4. Concluding remarks

The two new compounds described here enlarge the family of amine-templated lanthanum sulfates. Through this study, it is demonstrated that various structure topologies can be obtained by replacing only the amine group in the  $\text{La}_2(\text{SO}_4)_3 \cdot 8\text{H}_2\text{O}$ –amine– $\text{H}_2\text{SO}_4$ – $\text{H}_2\text{O}$  system. In addition to the 2D and 3D crystal structures described previously with ethylenediamine and piperazine, the first 1D lanthanum sulfate is attained by using diethylenetriamine as template and a 2D structure is built from dabco entities. In comparison with the previously reported amine-templated lanthanum sulfates, it is interesting to note that the lengthening of linear ethylenediamine to diethylenetriamine decreases the dimensionality of the structure from 2D to 1D. In the same way, by growing the cyclic piperazine to dabco, the dimensionality decreases from 3D to 2D. Then, it is of interest to chose appropriate amine entities to investigate the role of the size and the conformation of the templates in the construction of the crystal structures of lanthanide sulfates.

#### Acknowledgments

The authors thank Dr. T. Roisnel (Centre de Diffractométrie X, Université de Rennes I) and Mr. G. Marsolier for their assistance in single-crystal and powder X-ray diffraction data collection, respectively.

#### References

- [1] A.K. Cheetham, G. Férey, T. Loiseau, *Angew. Chem. Int. Ed.* 38 (1999) 3268–3292.
- [2] E. Jeanneau, N. Audebrand, D. Louër, *J. Mater. Chem.* 12 (2002) 2383–2389.
- [3] T. Conradsson, M.S. Dadachov, X.D. Zou, *Microporous Mesoporous Mater.* 41 (2000) 183–191.
- [4] S. Ekambaram, S.C. Sevov, *Inorg. Chem.* 39 (2000) 2405–2410 (and references therein).
- [5] G. Paul, A. Choudhury, C.N.R. Rao, *Dalton Trans.* 20 (2002) 3859–3867.
- [6] G. Paul, A. Choudhury, C.N.R. Rao, *Chem. Mater.* 15 (2003) 1174–1180.
- [7] A.J. Norquist, M.B. Doran, P.M. Thomas, D. O'Hare, *Dalton Trans.* 6 (2003) 1168–1175.
- [8] T. Bataille, D. Louër, *J. Mater. Chem.* 12 (2002) 3487–3493.
- [9] Y. Xing, Z. Shi, G. Li, W. Pang, *Dalton Trans.* 5 (2003) 940–943.
- [10] M.S. Wickleder, *Chem. Rev.* 102 (2002) 2011–2087.
- [11] J. Plévert, J.-P. Auffrédic, M. Louër, D. Louër, *J. Mater. Sci.* 24 (1989) 1913–1918.
- [12] Nonius, Kappa CCD Program Software, Nonius BV, Delft, The Netherlands, 1998.
- [13] Z. Otwinowski, W. Minor, in: C.W. Carter, R.M. Sweet (Eds.), *Methods in Enzymology*, Vol. 276, Academic Press, New York, 1997, pp. 307–326.
- [14] P. Coppens, in: F.R. Ahmed, S.R. Hall, C.P. Huber (Eds.), *Crystallographic Computing*, Munksgaard Publishers, Copenhagen, 1970, pp. 255–270.
- [15] A. Altomare, M.C. Burla, M. Camalli, G.L. Cascarano, C. Giacovazzo, A. Guagliardi, A.G.G. Moliterni, G. Polidori, R. Spagna, *J. Appl. Crystallogr.* 32 (1999) 115–119.
- [16] G.M. Sheldrick, *SHELXL-97: Program for Crystal Structure Refinement*, University of Göttingen, Germany, 1997.
- [17] L.J. Farrugia, *J. Appl. Crystallogr.* 32 (1999) 837–838.
- [18] R.E. Marsh, *Acta Crystallogr. B* 51 (1995) 897–907.
- [19] I.D. Brown, *J. Appl. Crystallogr.* 29 (1996) 479–480.
- [20] D. Louër, J. Rius, P. Bénard-Rocherullé, M. Louër, *Powder Diffract.* 16 (2001) 86–91 (and references therein).
- [21] I.D. Brown, *The Chemical Bond in Inorganic Chemistry: The Bond Valence Model*, IUCr Monographs on Crystallography, Vol. 12, Oxford University Press, Oxford, 2002, p. 80.
- [22] I.D. Brown, R.D. Shannon, *Acta Crystallogr. A* 29 (1973) 266–282.
- [23] P.M. Thomas, A.J. Norquist, M.B. Doran, D. O'Hare, *J. Mater. Chem.* 13 (2003) 88–92.
- [24] A.J. Norquist, P.M. Thomas, M.B. Doran, D. O'Hare, *Chem. Mater.* 14 (2002) 5179–5184.
- [25] C.L. Stuart, M.B. Doran, A.J. Norquist, D. O'Hare, *Acta Crystallogr. E* 59 (2003) m446–m448.
- [26] A. Choudhury, J. Krishnamoorthy, C.N.R. Rao, *Chem. Commun.* 24 (2001) 2610–2611.
- [27] G. Paul, A. Choudhury, R. Nagarajan, C.N.R. Rao, *Inorg. Chem.* 42 (2003) 2004–2013.
- [28] L. Niinistö, J. Toivonen, J. Valkonen, *Finn. Chem. Lett.* 3 (1980) 87–92.
- [29] N. Lah, I. Kralj Cigic, I. Leban, *Inorg. Chem. Commun.* 6 (2003) 1441–1444.
- [30] K. Jayaraman, A. Choudhury, C.N.R. Rao, *Solid State Sci.* 4 (2002) 413–422.
- [31] P. Bénard-Rocherullé, H. Tronel, D. Louër, *Powder Diffract.* 17 (2002) 210–217.
- [32] S. Govindarajan, K.C. Patil, H. Manohar, P.-E. Werner, *J. Chem. Soc. Dalton Trans.* 20 (1986) 119–123.
- [33] International Centre for Diffraction Data, *Powder Diffraction File*, Newtown Square, PA, 2002.